An insight into mitochondrial genomes of *Trichoderma afroharzianum* strains: a comparative and evolutionary analysis

Evrim ÖZKALEKAYA (evrimmiko@gmail.com)
Manisa Celal Bayar University: Manisa Celal Bayar Universitesi https://orcid.org/0000-0002-1707-9777
Özgül DOĞAN
Sivas Cumhuriyet Universitesi
Mahir BUDAK
Sivas Cumhuriyet Universitesi
Ertan Mahir KORKMAZ
Sivas Cumhuriyet Universitesi

Research Article

Keywords: mitochondrial genome, Trichoderma, biofungicide, hypocreales, genomic features, intron

Posted Date: October 11th, 2022

DOI: https://doi.org/10.21203/rs.3.rs-2132004/v1

Abstract

Trichoderma afroharzianum (Ascomycota: Hypocreales) is known as an important mycoparasite and biocontrol fungus and feeds on fungal material by parasitizing other fungi. Recent studies indicate that this species is also an ear rot pathogen in Europe. Here, the complete mitochondrial genome (mitogenome) of three *T. afroharzianum* strains was sequenced using next generation sequencing and comparatively characterised by the reported *Trichoderma* mitogenomes. *T. afroharzianum* mitogenomes were varying between 29,511 bp and 29,517 bp in length, with an average A + T content of 72.32%. These relatively compact mitogenomes contain 14 core PCGs, 22 tRNAs, two rRNAs, one gene encoding the ribosomal protein S3 and three or four genes including conserved domains for the homing endonucleases (HEGs; GIY-YIG type and LAGLIDADG type). All PCGs are initiated by ATG codons, except for *atp8*, and all are terminated with TAA as a stop codon. A significant correlation was observed between nucleotide composition and codon preference. Four introns belonging to the group I intron were predicted, accounting for about 14.54% of size of the mitogenomes. Phylogenetic analyses confirmed the positions of *T. afroharzianum* strains within the genus of *Trichoderma* and supported a sister relationship between *T. afroharzianum* and *T. harzianum* + *T. lixii*. The recovered trees also supported the monophyly of Nectriaceae, Bionectriaceae, Hypocreales incertea sedis, Cordycipitaceae and Hypocreaceae. However, Ophiocordycipitaceae and Clavicipitaceae were found to be paraphyletic.

1. Introduction

Members of the genus *Trichoderma* (Hypocreales), are widely used as biofungicides, biofertilizers, and as model fungi for the industrial production of plant biomass hydrolysing enzymes (CAZymes).The studies on the annotations and comparisons of nuclear and mitochondrial genomes of *Trichoderma* species have also recently been expanded in the directions of adaptation and evolution to gain a better understanding of their ecological traits, ecological roles for the more improved applications [e.g., biofungicide, biofertilizer, and producer of enzymes (CAZymes)] (Druzhinina et al., 2018; Kubicek et al., 2019, 2011; Martinez et al., 2008; Mukherjee et al., 2013; Schmoll et al., 2016). In a recent study by Fonseca et al., (2020), 788 curated mitogenomes representing 12 fungal phyla have been evaluated to assess discrepancies and similarities among them and to better understand the mechanisms involved in fungal mitogenome variability. Variations in the mitogenome length and composition are found mainly related to the number and length of accessory elements such as introns, HEGs, and unidentified ORFs. Accessory elements can also contribute to mitochondrial gene shuffling and mitogenome reorganization through promoting recombinational events (Zhang et al., 2021). Even so, the mitochondrial genome (mitogenome) of *Trichoderma* has relatively received much less attention despite mitochondria being the most necessary element for sustaining cell life (Kwak, 2021). We still have relatively limited knowledge about the common and unique patterns of mitogenome evolution in the economically important genus of *Trichoderma*. Although the genus includes more than 250 valid species based on molecular identification (Bissett et al., 2015), thus far (as of May 2022), complete or partial mitogenomes have only been reported for 11 isolates comprising seven species of *Trichoderma* (available as a verified dataset on GenBank).

The finding obtained from these reported mitogenomes demonstrated that adaptive evolution of the mitogenomes of *Trichoderma* has been actively ongoing concerning complex effects of various genetic elements (Fonseca et al., 2020; Kwak, 2021; Medina et al., 2020; Wallis et al., 2022). When considering the ecological features of fungi, such as a broad diversity of lineages and lifestyles in nature, all of the information on fungal mitogenomes can allow us to better understand the evolutionary adaptations and divergences, functional mechanisms in particular niches with both systematic and ecological perspectives of the *Trichoderma* in different environments.

As there is still a further requirement to increase the number of representative mitogenomes from *Trichoderma*, we here sequenced and characterised the complete mitogenome of three *Trichoderma afroharzianum* (Ascomycota: Hypocreales) strains for the first time. This species is known as an important mycoparasite and biocontrol fungus and feeds on fungal material by parasitizing other fungi. However, recent studies also show that this species is an ear rot pathogen in Europe (Pfordt et al., 2020; Sanna et al., 2022). We have also compared these mitogenomes with the previously reported mitogenomes of *Trichoderma* for a better understanding of the mitogenome architectures and features of this genus. Finally, we have carried out phylogenetic analyses to confirm the phylogenetic position of *T. afroharzianum* using a mitogenome dataset of 58 species of Hypocreales (Ascomycota: Sordariomycetes).

2. Materials And Methods

2.1 Strains, DNA extraction and mitogenome sequencing

Three strains from *T. afroharzianum* were provided from Fundamental and Industrial Microbiology Laboratory of Manisa Celal Bayar University (Türkiye). The fungi were cultured on potato dextrose agar (PDA, Merck) at 27°C for seven days. Total genomic DNA of each sample was then extracted from the mycelia from the surface of the media using a modified sodium dodecyl sulphate/phenol protocol developed by Vazquez-Angulo et al. (2012). The genomic DNA extract of each sample was quantified using a Qubit™ 4.0 Fluorometer (ThermoFisher Scientific, USA), and 100 ng of each was then pooled and sequenced using the Illumina MiSeq next-generation sequencing (NGS) platform using 300 bp paired-end reads, conducted at Advanced Technology Application and Research Centre of Sivas Cumhuriyet University (CUTAM, Türkiye).

2.2 Mitogenome assembly, annotation and analyses

Raw NGS reads of each sample were processed by trimming adapter sequences and filtering low quality reads which have low quality scores (< 20) or poly-Ns (> 5 bp Ns) using fastp v0.20.0 (Chen et al., 2018). The filtered clean reads were then imported into Geneious R9 (Kearse et al., 2012). The reads were assembled into contigs using two different approaches for constructing the mitogenome of each sample: (i) reference assembly using the mitogenomes of *T. harzianum* (accession numbers: MN564945, MZ713368) under the parameters of ‘medium–low sensitivity’ and ‘iterate up to five times’; (ii) *de novo* assemblies of the sequences using MIRA assembler implemented in Geneious R9 and then mapping the

obtained contigs to the mitogenomes produced under the first approach. The generated contigs from both approaches were then aligned, compared, and finally compiled into a single assembly for each sample.

The annotations of the obtained *T. afroharzianum* mitogenomes were performed using MFannot (https://megasun.bch.umontreal.ca/cgi-bin/mfannot/mfannotInterface.pl) (Valach et al., 2014) and MITOS web servers (http://mitos.bioinf.uni-leipzig.de/index.py) (Bernt et al., 2013) under the Mold, Protozoan, and Coelenterate Mitochondrial Genetic Code. The boundaries of PCGs were then refined by using BLAST searches against NCBI non-redundant (nr) database (O'Leary et al., 2016) and NCBI ORF Finder (https://www.ncbi.nlm.nih.gov/orffinder), and comparing manually with those of *T. harzianum* mitogenomes. tRNA genes were annotated using the combination of tRNAscan-SE (Chan and Lowe, 2019) and RNAweasel (https://megasun.bch.umontreal.ca/cgi-bin/RNAweasel/RNAweaselInterface.pl) (Lang et al., 2007) web servers under the Genetic Code 4. The mitochondrial intron sequences and their types were predicted using RNAweasel and MFannot web servers. Additionally, intergenic and overlapping regions between genes were determined manually. The repetitive regions in the mitogenomes of *T. afroharzianum* were investigated using Tandem Repeats Finder (https://tandem.bu.edu/trf/trf.html) (Benson, 1999). Finally, the visualization of the circular mitogenome was performed using OrganellarGenomeDRAW (OGDRAW) (Greiner et al., 2019). The complete mitogenome sequences of *T. afroharzianum* were deposited into GenBank under the accession numbers ON764437 - ON764439.

The basic nucleotide compositions, average nucleotide and amino acid divergences, and codon usage bias of the *T. afroharzianum* mitogenomes were computed using MEGA v7.0 (Kumar et al., 2016). The strand asymmetric bias of the nucleotide composition was calculated according to the following formulae: AT-skew = (A – T) / (A + T) and GC-skew = (G – C) / (G + C) (Perna and Kocher, 1995).

2.3 Phylogenetic and comparative analyses

Phylogenetic and comparative analyses were performed using the mitogenome dataset of 58 Hypocreales (Ascomycota: Sordariomycetes) species representing seven families, and using *Neurospora crassa* (strain OR74A) from Sordariales as outgroup (Table S1). The nucleotide sequences of the 14 mitochondrial protein coding genes (*atp6*, *atp8*, *atp9, cob*, *cox1*, *cox2*, *cox3*, *nad1*, *nad2*, *nad3*, *nad4*, *nad4L*, *nad5* and nad6) were used in the phylogenetic analyses. All of the PCGs were aligned individually with MAFFT (Katoh and Standley, 2013) implemented in PhyloSuite v1.2.2 (Zhang et al., 2020) using the L-INS-i algorithm and codon alignment mode. The aligned sequences were then concatenated using "Concatenate Sequence" function of PhyloSuite. The best-fit partitioning scheme and evolutionary models were selected by PartitionFinder 2 (Lanfear et al., 2017) using the "greedy" algorithm with the option of "unlinked" branch lengths and the Bayesian Information Criterion (BIC). The optimal partitioning scheme and determined models were used in subsequent phylogenetic analyses (Table S2). Phylogenetic analyses were performed using both Maximum Likelihood (ML) and Bayesian inference (BI) approaches. The ML tree was inferred using IQ-Tree (Nguyen et al., 2015) under the model selected by PartitionFinder 2 with 1000 ultrafast (Minh et al., 2013) bootstraps, as well as the Shimodaira–Hasegawa–like approximate likelihood-ratio test (Guindon et al., 2010). The BI tree was reconstructed using MrBayes

v3.2.6 (Ronquist et al., 2012) with two independent runs of 10 million generations with four Markov chains (three heated chains and one cold chain) and sampling every 1,000 generations. The stationarity of the chains was assessed using Tracer v1.7 (Rambaut et al., 2018), and then the first 25% of trees in each run were discarded as burn-in and a majority-rule consensus tree (BI tree) was generated from the remaining trees. The consensus phylogenetic trees were visualized using FigTree v1.4.2 (Rambaut, 2014).

3. Results And Discussion

Mitogenomic features and nucleotide composition

Three complete mitogenomes from *T. afroharzianum* were obtained with the lengths ranging from 29,511 bp (strains of TR43 and TR47) to 29,517 bp (strain of TR37) (Fig. 1 and Table 1 and Table S3). The sizes of the mitogenomes were within the range of those of other reported *Trichoderma* mitogenomes, which are varying between 27,631 bp in *T. harzianum* (Wallis et al., 2022) and 94,608 bp in *T. cornu-damae strain* KA19-0412C (GenBank accession no. MW525445). The observed variation in mitogenome size among both *Trichoderma* species and the other members of the Hypocreales order reported to date may be mainly attributable to the differences in length and number of introns, homing endonucleases and putative ORFs (Fonseca et al., 2020; Ren et al., 2021; Yuan et al., 2017; Zhang et al., 2015). However, the mitogenome architectures of *T. afroharzianum* were closely consistent with those of previously reported *Trichoderma* mitogenomes (Chung et al., 2022; Fonseca et al., 2020; Kwak, 2021, 2020; Li et al., 2021; Medina et al., 2020; Wallis et al., 2022), comprising 14 core PCGs, 22 tRNAs, two rRNAs, one gene encoding the ribosomal protein S3 and three or four genes including conserved domains for the homing endonucleases (HEGs; GIY-YIG type and LAGLIDADG type) (Fig. 1 and Table 1 and Table S3). The mitogenomes of *T. afroharzianum* TR37 and TR47 were additionally containing one open reading frame (orf148) encoding a hypothetical protein. All of the identified genes were located on the heavy strand (H-strand) (Figure 1). These mitogenomes seem to be relatively compact, with genic regions harbouring intronic regions accounting for ~81.85% and intergenic regions accounting for ~18.15% of the whole mitogenomes (Table 1).

Similar to the reported fungal mitogenomes characterized by a high AT content (Medina et al., 2020), the nucleotide compositions of the obtained mitogenomes were biased towards A and T, with an average 72.32% A+T content (Table 2). An AT bias was also found in all PCGs of three mitogenomes (72.29%, Table 2). The bias in nucleotide composition was also evaluated by analysing the codon positions separately (Table 2). The A+T content of the third codon position (85.58%) was higher than those of the second (66.14%) and first codon positions (65.18%), designating the reduced effect of selective forces acting on the nucleotides at the third codon position. Furthermore, the bias level of nucleotide ‘T’ usage is highest in the second codon position (44.67% T content on average), which reveal that this bias might be explained by the mutational pressure forced by the strong preference of mitochondrial proteins in favour of non-polar and hydrophobic amino acids with codons having a T at this codon positon (Doğan and Korkmaz, 2017). As for the skews, the slightly negative AT and moderately positive GC skews were observed in whole genomes (-0.0017 and 0.0959, Table 3), indicating an excess of T relative to A and an

excess of G relative to C, respectively. However, a deviation towards the nucleotide A was observed in both the first and third codon positions of PCGs (0.0043 and 0.0644, respectively). This deviation might be related with variable influences of the selection pressures acting on the codon positions of the PCGs (Aydemir and Korkmaz, 2020).

Protein coding genes and codon usage

The total length of the 14 conserved protein coding genes was 14,307 bp, accounting for about 48.5% of the complete mitogenomes (Table 1). These genes were composed of three ATP synthases (*atp6*, *atp8*, and *atp9*), three cytochrome c oxidases (*cox1*, *cox2*, and *cox3*), one apocytochrome b (*cob*), and seven NADH dehydrogenases (*nad1*, *nad2*, *nad3*, *nad4*, *nad4L*, *nad5*, and *nad6*). The orf148 was determined to be a form of freestanding ORF with a length of 447 bp. The lengths of PCGs were conserved and of these genes, the *cox1* is highest (2838 bp) and *atp8* is the shortest (153 bp). All of the conserved genes and orf148 were found to have ATG as the predicted initiation codon and TAA as the termination codon, except for *atp8*, which had an ATA initiation codon. As commonly seen in both *Trichoderma* and Hypocreales mitogenomes (Chambergo et al., 2002; Fonseca et al., 2020; Kwak, 2021; Ren et al., 2021; Venice et al., 2020), an overlap of one nucleotide base was detected between the TAA stop codon of *nad4L* and the ATG start codon of *nad5* (-1 bp, corresponding to the codon of A).

Comparisons of the relative synonymous codon usage (RSCU) of *T. afroharzianum* mitogenomes indicated that almost all amino acids displayed codon usage bias (Fig. 2, Table S4) and reflected a significant correlation between nucleotide composition and codon preference. Leucine (L) was the most abundant amino acid (with a relative frequency of 14.54%), while Cys (C) is the least common (0.53%). Additionally, UUA-Leu, AUA-Met, UUU-Phe, GUA-Val and UUC-Phe were the most frequently preferred codons. The total content of these five codons were approximately 32.20%, similar to that of other *Trichoderma* species (Kwak, 2020). However, the codons rich in C and G, such as UGG-Trp, CCG-Pro, CGC-Arg, GGC-Gly, GCG-Ala and ACG-Thr, were absent or rarely used in these mitogenomes (Fig. 2; Table S4).

Transfer RNA and ribosomal RNA genes

The total length of the 22 tRNA genes was 1,640 bp, accounting for ~ 5.56% of the size of the complete mitogenomes. Their size was ranged from 71 bp to 84 bp (Table 1, Table S3), with an A+T content of 60.20% on average. All of the 22 tRNAs was found to be free-standing on the H-strand, with mostly a usual clover-leaf secondary structure. As commonly observed in fungal mitogenomes (Medina et al., 2020), most of the tRNAs were found as single copies, however, three tRNAs were predicted in multiple copies with same and/or different anticodons [three copies for *trnM* with same anticodon (*trnM*-CAT)), two copies for *trnR* (*trnR*-ACG and *trnR*-TCT) and two copies for *trnL* (*trnL*-TAA and *trnL*-TAG); Table 1, Table S3). The lengths of *rrnS* and *rrnL* genes were 1502 bp and 5422 bp, respectively, accounting for approximately 23.46% of the entire size of three mitogenomes, with an A+T content of 70.75% on average (Table 2). Their lengths were in a comparable range to homologous genes in other known *Trichoderma* species (Chung et al., 2022; Kwak, 2021). The *rrnS* gene was positioned between *atp6* and *trnY* genes as

a free-standing ORF, but the *rrnL* gene was located between *trnP* and *trnT* genes in a position ranging over both homing endonuclease (LAGLIDADG) and *rps3* (Fig. 1, Table 1).

Intronic and intergenic regions

The intronic sequences, which are known as one of the features contributing size expansion and structural variability in the fungal mitogenomes (Haugen et al., 2005; Hurst and Werren, 2001; Kanzi et al., 2016; Kwak, 2020), were investigated in *T. afroharzianum* mitogenomes and analysed by comparison with those of other reported *Trichoderma* species. These mitochondrial introns are divided into two groups as group I and group II based on their nucleotide sequences, conserved secondary structures and splicing mechanisms (Lang et al., 2007; Zhang and Zhang, 2019) that are known to have a major role in genome evolution (Schuster et al., 2017). The loop regions of group I and II introns also harbour ORFs that encoded different site-specific homing endonuclease (HE) genes (Schäfer, 2003). Of these, the group I introns as the most abundant introns in fungal mitogenomes are considered to be mobile genetic elements, which are frequently inserted within different mitochondrial genes, particularly protein coding genes and rRNA genes (Edgell et al., 2011; Paquin et al., 1997). Here, four introns belonging to the group I intron were predicted in the mitogenomes of *T. afroharzianum* (Fig. 3), accounting for ~ 13.60% of the size of the mitogenomes. Of these, the first intron with a length of 1245 bp was predicted in the exon-intron structure of *cox1* gene and exhibited 98.96% identity (100% query coverage, E value = 0.0) with an intergenic region between cytochrome p450 and GMC oxidoreductase genes of *Trichoderma simmonsii* strain GH-Sj1 (CP_075866) and and 90.54%% identity with the intron in cox1 gene of *Ophiostoma himal-ulmi* strain CBS 374.67 (Ophiostomatales) (99% query coverage, E value = 0.0; MW250274), which classified in the subtype of IB. This intron was predicted to harbour an ORF corresponding to the GIY-YIG motif of the HE protein. The second intron was also classified as the subtype of IB with a length of 895 bp in the *rrnL* gene and had high identity (94.65%) with the intron 1B in the *rrnL* gene of *Cordyceps chanhua* isolate JGS-7 (MH_734937). This intron was also predicted to harbour an ORF corresponding to the LAGLIDADG motif of the HE protein. The third intron (classified as the subtype of IA) was predicted in the *rrnL* gene with a length of 1641 bp and exhibited 98.72% identity with the intron sequence in the *rrnL* gene of three *Trichoderma* species (NC_052832, MZ292901). The *rps3* gene encoding 40S ribosomal protein S3 was predicted to be located within this intron as an internal ORF of the *rrnL* gene, which is a commonly observed pattern in the fungal mitogenomes (Kwak, 2020; Lang et al., 2007; Wai et al., 2019). The last intron (classified as the subtype of IC2) with a length of 232 bp was found within an ORF consisting of either the putative maturase or the LAGLIDADG motif of the HE protein (Fig. 3). This intron displayed high identity (91.44 - 99.55%) with those of other *Trichoderma* mitogenomes (CP071114, NC_003388, MF287973, MW525445).

Despite the variability in total length of intergenic regions, *T. afroharzianum* mitogenomes displayed the relatively high coding density, a general feature of mitogenome evolution, probably by the key contribution of reductive evolution on the non-coding regions. The total length of the intergenic regions was 5274 bp (at 35 sites and 17.87% of the complete mitogenome) in *T. afroharzianum* TR43 and 5453 bp (at 36 sites and 18.48% of the complete mitogenomes) in *T. afroharzianum* TR37 and TR47, with size

of 4-581 bp (Table 1, Table S1). The longest was located between *atp6* and *rrnS* genes. Homology searches on the longest intergenic region of *T. afroharzianum* revealed significant similarity to those of other reported *Trichoderma* species with a range of between 97.42% and 89.74% homology. The rate of the total size of intergenic regions to total length of the mitogenomes was within the range of those of other reported *Trichoderma* mitogenomes, which is varying between 16.50% in *T. koningiopsis POS7* (MT816499) and 24.93% in *T. atroviride* ATCC 26799 (Kwak, 2020).

Phylomitogenomic of the T. afroharzianum within the order Hypocreales

The identical and well supported phylogenetic relationships were recovered in both tree topologies (Fig. 4). The obtained topology was also not sensitive to inference approach. The recovered trees confirmed the taxonomic positions of *T. afroharzianum* TR37, TR43 and TR47 within the genus of *Trichoderma* and supported a sister group relationship between *T. afroharzianum* and *T. harzianum* + *T. lixii*. The monophyly of the genus of *Trichoderma* was also supported, consistent with the most of the previously reported phylogenies (Chung et al., 2022; Kwak, 2021, 2020). In the Hypocreales, the recovered trees supported the monophyly of Nectriaceae, Bionectriaceae, Hypocreales incertea sedis, Cordycipitaceae and Hypocreaceae. However, the Ophiocordycipitaceae and Clavicipitaceae was found to be paraphyletic (Fig. 4). The occurrence of paraphyletic relationship between these two families has also been reported by Kwak (2020), clearly indicating the requirement for new mitogenomes from unreported Hypocreales families/genera, particularly from Ophiocordycipitaceae, Clavicipitaceae and Bionectriaceae.

Declarations

Declaration of Competing Interest

The authors declare that they have no known competing financial interests or personal relationships that could have appeared to influence the work reported in this paper.

Acknowledgement

This study was supported by the Manisa Celal Bayar University Scientific Research Commission Unit under the grant number 2020-022. We present our gratitudes to the staff of Sivas Cumhuriyet University Evolutionary Bioinformatics Research Group (EBRG) for their help in every stages of laboratory work.

References

Aydemir, M.N., Korkmaz, E.M., 2020. Comparative mitogenomics of Hymenoptera reveals evolutionary differences in structure and composition. Int. J. Biol.
Macromol. https://doi.org/10.1016/j.ijbiomac.2019.12.135.

Benson, G., 1999. Tandem repeats finder: A program to analyze DNA sequences. Nucleic Acids Res. 27, 573–580. https://doi.org/10.1093/nar/27.2.573.

Bernt, M., Donath, A., Jühling, F., Externbrink, F., Florentz, C., Fritzsch, G., Pütz, J., Middendorf, M., Stadler, P.F., 2013. MITOS: Improved de novo metazoan mitochondrial genome annotation. Mol. Phylogenet. Evol. 69, 313–319. https://doi.org/10.1016/j.ympev.2012.08.023.

Bissett, J., Gams, W., Jaklitsch, W., Samuels, G.J., 2015. Accepted *Trichoderma* names in the year 2015. IMA Fungus 6, 263–295. https://doi.org/10.5598/imafungus.2015.06.02.02.

Chambergo, F.S., Bonaccorsi, E.D., Ferreira, A.J.S., Ramos, A.S.P., Ferreira, J.R., Abrahão-Neto, J., Farah, J.P.S., El-Dorry, H., 2002. Elucidation of the metabolic fate of glucose in the filamentous fungus *Trichoderma reesei* using expressed sequence Tag (EST) analysis and cDNA microarrays. J. Biol. Chem. 277, 13983–13988. https://doi.org/10.1074/jbc.M107651200.

Chan, P.P., Lowe, T.M., 2019. tRNAscan-SE: Searching for tRNA genes in genomic sequences. Methods Mol. Biol. 1962, 1. https://doi.org/10.1007/978-1-4939-9173-0_1.

Chen, S., Zhou, Y., Chen, Y., Gu, J., 2018. fastp: An ultra-fast all-in-one FASTQ preprocessor. Bioinformatics. 34, i884–i890. https://doi.org/10.1093/bioinformatics/bty560.

Chung, D., Kwon, Y.M., Yang, Y., 2022. The complete mitochondrial genome of *Trichoderma simmonsii* (Hypocreales: Hypocreaceae) from the Southern Coast of Korea. Mitochondrial DNA Part B. 7, 640–641. https://doi.org/10.1080/23802359.2022.2060766.

Doğan, Ö., Korkmaz, E.M., 2017. Nearly complete mitogenome of hairy sawfly, Corynis lateralis (Brullé, 1832) (Hymenoptera: Cimbicidae): rearrangements in the IQM and ARNS1EF gene clusters. Genetica. 145, 341–350. https://doi.org/10.1007/s10709-017-9969-7.

Druzhinina, I.S., Chenthamara, K., Zhang, J., Atanasova, L., Yang, D., Miao, Y., Rahimi, M.J., Grujic, M., Cai, F., Pourmehdi, S., Salim, K.A., Pretzer, C., Kopchinskiy, A.G., Henrissat, B., Kuo, A., Hundley, H., Wang, M., Aerts, A., Salamov, A., Lipzen, A., LaButti, K., Barry, K., Grigoriev, I.V., Shen, Q., Kubicek, C.P., 2018. Massive lateral transfer of genes encoding plant cell wall-degrading enzymes to the mycoparasitic fungus *Trichoderma* from its plant-associated hosts. PLOS Genet. 14, e1007322. https://doi.org/10.1371/journal.pgen.1007322.

Edgell, D.R., Chalamcharla, V.R., Belfort, M., 2011. Learning to live together: Mutualism between self-splicing introns and their hosts. BMC Biol. 9, 22. https://doi.org/10.1186/1741-7007-9-22.

Fonseca, P.L.C., Badotti, F., De-Paula, R.B., Araújo, D.S., Bortolini, D.E., Del-Bem, L.-E., Azevedo, V.A., Brenig, B., Aguiar, E.R.G.R., Góes-Neto, A., 2020. Exploring the relationship among divergence time and coding and non-coding elements in the shaping of fungal mitochondrial genomes. Front. Microbiol. 11, 765. https://doi.org/10.3389/fmicb.2020.00765.

Greiner, S., Lehwark, P., Bock, R., 2019. OrganellarGenomeDRAW (OGDRAW) version 1.3.1: Expanded toolkit for the graphical visualization of organellar genomes. Nucleic Acids Res. 47, W59–W64. https://doi.org/10.1093/nar/gkz238.

Guindon, S., Dufayard, J.F., Lefort, V., Anisimova, M., Hordijk, W., Gascuel, O., 2010. New algorithms and methods to estimate maximum-likelihood phylogenies: Assessing the performance of PhyML 3.0. Syst. Biol. 59, 307–321. https://doi.org/10.1093/sysbio/syq010.

Haugen, P., Simon, D.M., Bhattacharya, D., 2005. The natural history of group I introns. Trends Genet. 21, 111–119. https://doi.org/10.1016/j.tig.2004.12.007.

Hurst, G.D.D., Werren, J.H., 2001. The role of selfish genetic elements in eukaryotic evolution. Nat. Rev. Genet. 2, 597–606. https://doi.org/10.1038/35084545.

Kanzi, A.M., Wingfield, B.D., Steenkamp, E.T., Naidoo, S., van der Merwe, N.A., 2016. Intron derived size polymorphism in the mitochondrial genomes of closely related *Chrysoporthe* species. PLoS One. 11, e0156104. https://doi.org/10.1371/journal.pone.0156104.

Katoh, K., Standley, D.M., 2013. MAFFT multiple sequence alignment software version 7: Improvements in performance and usability. Mol. Biol. Evol. 30, 772–80. https://doi.org/10.1093/molbev/mst010.

Kearse, M., Moir, R., Wilson, A., Stones-Havas, S., Cheung, M., Sturrock, S., Buxton, S., Cooper, A., Markowitz, S., Duran, C., Thierer, T., Ashton, B., Meintjes, P., Drummond, A., 2012. Geneious Basic: An integrated and extendable desktop software platform for the organization and analysis of sequence data. Bioinformatics. 28, 1647–9. https://doi.org/10.1093/bioinformatics/bts199.

Kubicek, C.P., Herrera-Estrella, A., Seidl-Seiboth, V., Martinez, D.A., Druzhinina, I.S., Thon, M., Zeilinger, S., Casas-Flores, S., Horwitz, B.A., Mukherjee, P.K., Mukherjee, M., Kredics, L., Alcaraz, L.D., Aerts, A., Antal, Z., Atanasova, L., Cervantes-Badillo, M.G., Challacombe, J., Chertkov, O., McCluskey, K., Coulpier, F., Deshpande, N., von Döhren, H., Ebbole, D.J., Esquivel-Naranjo, E.U., Fekete, E., Flipphi, M., Glaser, F., Gómez-Rodríguez, E.Y., Gruber, S., Han, C., Henrissat, B., Hermosa, R., Hernández-Oñate, M., Karaffa, L., Kosti, I., Le Crom, S., Lindquist, E., Lucas, S., Lübeck, M., Lübeck, P.S., Margeot, A., Metz, B., Misra, M., Nevalainen, H., Omann, M., Packer, N., Perrone, G., Uresti-Rivera, E.E., Salamov, A., Schmoll, M., Seiboth, B., Shapiro, H., Sukno, S., Tamayo-Ramos, J.A., Tisch, D., Wiest, A., Wilkinson, H.H., Zhang, M., Coutinho, P.M., Kenerley, C.M., Monte, E., Baker, S.E., Grigoriev, I.V., 2011. Comparative genome sequence analysis underscores mycoparasitism as the ancestral life style of *Trichoderma*. Genome Biol. 12, R40. https://doi.org/10.1186/gb-2011-12-4-r40.

Kubicek, C.P., Steindorff, A.S., Chenthamara, K., Manganiello, G., Henrissat, B., Zhang, J., Cai, F., Kopchinskiy, A.G., Kubicek, E.M., Kuo, A., Baroncelli, R., Sarrocco, S., Noronha, E.F., Vannacci, G., Shen, Q., Grigoriev, I.V., Druzhinina, I.S., 2019. Evolution and comparative genomics of the most common *Trichoderma* species. BMC Genomics. 20. https://doi.org/10.1186/s12864-019-5680-7.

Kumar, S., Stecher, G., Tamura, K., 2016. MEGA7: Molecular evolutionary genetics analysis version 7.0 for bigger datasets. Mol. Biol. Evol. 33, 1870–4. https://doi.org/10.1093/molbev/msw054.

Kwak, Y., 2021. An update on *Trichoderma* mitogenomes: Complete de novo mitochondrial genome of the fungal biocontrol agent *Trichoderma harzianum* (Hypocreales, Sordariomycetes), an ex-neotype strain CBS 226.95, and tracing the evolutionary divergences of mitogenomes in *Trichoderma*. Microorganisms. 9. https://doi.org/10.3390/microorganisms9081564.

Kwak, Y., 2020. Complete mitochondrial genome of the fungal biocontrol agent *Trichoderma atroviride:* Genomic features, comparative analysis and insight into the mitochondrial evolution in *Trichoderma*. Front. Microbiol. 11, 785. https://doi.org/10.3389/fmicb.2020.00785.

Lanfear, R., Frandsen, P.B., Wright, A.M., Senfeld, T., Calcott, B., 2017. PartitionFinder 2: New methods for selecting partitioned models of evolution for molecular and morphological phylogenetic analyses. Mol. Biol. Evol. 34, 772–773. https://doi.org/10.1093/molbev/msw260.

Lang, B.F., Laforest, M.J., Burger, G., 2007. Mitochondrial introns: A critical view. Trends Genet. 23, 119–125. https://doi.org/10.1016/J.TIG.2007.01.006.

Li, W.-C., Lin, T.-C., Chen, C.-L., Liu, H.-C., Lin, H.-N., Chao, J.-L., Hsieh, C.-H., Ni, H.-F., Chen, R.-S., Wang, T.-F., 2021. Complete genome sequences and genome-wide characterization of *Trichoderma* biocontrol agents provide new insights into their evolution and variation in genome organization, sexual development, and fungal-plant interactions. Microbiol. Spectr. 9, e0066321. https://doi.org/10.1128/Spectrum.00663-21.

Martinez, D., Berka, R.M., Henrissat, B., Saloheimo, M., Arvas, M., Baker, S.E., Chapman, J., Chertkov, O., Coutinho, P.M., Cullen, D., Danchin, E.G.J., Grigoriev, I.V, Harris, P., Jackson, M., Kubicek, C.P., Han, C.S., Ho, I., Larrondo, L.F., de Leon, A.L., Magnuson, J.K., Merino, S., Misra, M., Nelson, B., Putnam, N., Robbertse, B., Salamov, A.A., Schmoll, M., Terry, A., Thayer, N., Westerholm-Parvinen, A., Schoch, C.L., Yao, J., Barabote, R., Nelson, M.A., Detter, C., Bruce, D., Kuske, C.R., Xie, G., Richardson, P., Rokhsar, D.S., Lucas, S.M., Rubin, E.M., Dunn-Coleman, N., Ward, M., Brettin, T.S., 2008. Genome sequencing and analysis of the biomass-degrading fungus *Trichoderma reesei* (syn. Hypocrea jecorina). Nat. Biotechnol. 26, 553–560. https://doi.org/10.1038/nbt1403.

Medina, R., Franco, M.E.E., Bartel, L.C., Martinez Alcántara, V., Saparrat, M.C.N., Balatti, P.A., 2020. Fungal mitogenomes: Relevant features to planning plant disease management. Front. Microbiol. 11, 978. https://doi.org/10.3389/fmicb.2020.00978.

Minh, B.Q., Nguyen, M.A.T., von Haeseler, A., 2013. Ultrafast approximation for phylogenetic bootstrap. Mol. Biol. Evol. 30, 1188–1195. https://doi.org/10.1093/molbev/mst024.

Mukherjee, P.K., Horwitz, B.A., Herrera-Estrella, A., Schmoll, M., Kenerley, C.M., 2013. *Trichoderma* research in the genome era. Annu. Rev. Phytopathol. 51, 105–129. https://doi.org/10.1146/annurev-phyto-082712-102353.

Nguyen, L.T., Schmidt, H.A., Von Haeseler, A., Minh, B.Q., 2015. IQ-TREE: A fast and effective stochastic algorithm for estimating maximum-likelihood phylogenies. Mol. Biol. Evol. https://doi.org/10.1093/molbev/msu300.

O'Leary, N.A., Wright, M.W., Brister, J.R., Ciufo, S., Haddad, D., McVeigh, R., Rajput, B., Robbertse, B., Smith-White, B., Ako-Adjei, D., Astashyn, A., Badretdin, A., Bao, Y., Blinkova, O., Brover, V., Chetvernin, V., Choi, J., Cox, E., Ermolaeva, O., Farrell, C.M., Goldfarb, T., Gupta, T., Haft, D., Hatcher, E., Hlavina, W., Joardar, V.S., Kodali, V.K., Li, W., Maglott, D., Masterson, P., McGarvey, K.M., Murphy, M.R., O'Neill, K., Pujar, S., Rangwala, S.H., Rausch, D., Riddick, L.D., Schoch, C., Shkeda, A., Storz, S.S., Sun, H., Thibaud-Nissen, F., Tolstoy, I., Tully, R.E., Vatsan, A.R., Wallin, C., Webb, D., Wu, W., Landrum, M.J., Kimchi, A., Tatusova, T., DiCuccio, M., Kitts, P., Murphy, T.D., Pruitt, K.D., 2016. Reference sequence (RefSeq) database at NCBI: Current status, taxonomic expansion, and functional annotation. Nucleic Acids Res. 44, D733-45. https://doi.org/10.1093/nar/gkv1189.

Paquin, B., Laforest, M.-J., Forget, L., Roewer, I., Wang, Z., Longcore, J., Lang, B.F., 1997. The fungal mitochondrial genome project: Evolution of fungal mitochondrial genomes and their gene expression. Curr. Genet. 31, 380–395. https://doi.org/10.1007/s002940050220.

Perna, N.T., Kocher, T.D., 1995. Patterns of nucleotide composition at fourfold degenerate sites of animal mitochondrial genomes. J. Mol. Evol. 41, 353–358. https://doi.org/10.1007/BF01215182.

Pfordt, A., Schiwek, S., Karlovsky, P., von Tiedemann, A., 2020. *Trichoderma afroharzianum* ear rot–a new disease on maize in Europe. Front. Agron. 2. https://doi.org/10.3389/fagro.2020.547758.

Rambaut, A., 2014. FigTree v1.4.2, a graphical viewer of phylogenetic trees. available from http//tree.bio.ed.ac.uk/software/figtree/.

Rambaut, A., Drummond, A.J., Xie, D., Baele, G., Suchard, M.A., 2018. Posterior summarization in bayesian phylogenetics using tracer 1.7. Syst. Biol. 67, 901–904. https://doi.org/10.1093/sysbio/syy032.

Ren, L.-Y., Zhang, S., Zhang, Y.-J., 2021. Comparative mitogenomics of fungal species in Stachybotryaceae provides evolutionary insights into Hypocreales. Int. J. Mol. Sci. 22, 13341. https://doi.org/10.3390/ijms222413341.

Ronquist, F., Teslenko, M., Van Der Mark, P., Ayres, D.L., Darling, A., Höhna, S., Larget, B., Liu, L., Suchard, M.A., Huelsenbeck, J.P., 2012. Mrbayes 3.2: Efficient bayesian phylogenetic inference and model choice across a large model space. Syst. Biol. 61, 539–542. https://doi.org/10.1093/sysbio/sys029.

Sanna, M., Pugliese, M., Gullino, M.L., Mezzalama, M., 2022. First report of *Trichoderma afroharzianum* causing seed rot on maize in Italy. Plant Dis. https://doi.org/10.1094/PDIS-12-21-2697-PDN.

Schäfer, B., 2003. Genetic conservation versus variability in mitochondria: the architecture of the mitochondrial genome in the petite-negative yeast *Schizosaccharomyces pombe*. Curr. Genet. 43, 311–

326. https://doi.org/10.1007/s00294-003-0404-5.

Schmoll, M., Dattenböck, C., Carreras-Villaseñor, N., Mendoza-Mendoza, A., Tisch, D., Alemán, M.I., Baker, S.E., Brown, C., Cervantes-Badillo, M.G., Cetz-Chel, J., Cristobal-Mondragon, G.R., Delaye, L., Esquivel-Naranjo, E.U., Frischmann, A., Gallardo-Negrete, J. de J., García-Esquivel, M., Gomez-Rodriguez, E.Y., Greenwood, D.R., Hernández-Oñate, M., Kruszewska, J.S., Lawry, R., Mora-Montes, H.M., Muñoz-Centeno, T., Nieto-Jacobo, M.F., Nogueira Lopez, G., Olmedo-Monfil, V., Osorio-Concepcion, M., Piłsyk, S., Pomraning, K.R., Rodriguez-Iglesias, A., Rosales-Saavedra, M.T., Sánchez-Arreguín, J.A., Seidl-Seiboth, V., Stewart, A., Uresti-Rivera, E.E., Wang, C.-L., Wang, T.-F., Zeilinger, S., Casas-Flores, S., Herrera-Estrella, A., 2016. The genomes of three uneven siblings: Footprints of the lifestyles of three *Trichoderma* species. Microbiol. Mol. Biol. Rev. 80, 205–327. https://doi.org/10.1128/MMBR.00040-15.

Schuster, A., Lopez, J.V., Becking, L.E., Kelly, M., Pomponi, S.A., Wörheide, G., Erpenbeck, D., Cárdenas, P., 2017. Evolution of group I introns in Porifera: New evidence for intron mobility and implications for DNA barcoding. BMC Evol. Biol. 17, 82. https://doi.org/10.1186/s12862-017-0928-9.

Valach, M., Burger, G., Gray, M.W., Lang, B.F., 2014. Widespread occurrence of organelle genome-encoded 5S rRNAs including permuted molecules. Nucleic Acids Res. 42, 13764–77. https://doi.org/10.1093/nar/gku1266.

Vazquez-Angulo, J.C., Mendez-Trujillo, V., González-Mendoza, D., Morales-Trejo, A., Grimaldo-Juarez, O., Cervantes-Díaz, L., 2012. A rapid and inexpensive method for isolation of total DNA from *Trichoderma* spp (Hypocreaceae). Genet. Mol. Res. 11, 1379–1384. https://doi.org/10.4238/2012.May.15.8.

Venice, F., Davolos, D., Spina, F., Poli, A., Prigione, V.P., Varese, G.C., Ghignone, S., 2020. Genome sequence of *Trichoderma lixii* MUT3171, a promising strain for mycoremediation of PAH-contaminated sites. Microorganisms. 8. https://doi.org/10.3390/microorganisms8091258.

Wai, A., Shen, C., Carta, A., Dansen, A., Crous, P.W., Hausner, G., 2019. Intron-encoded ribosomal proteins and N-acetyltransferases within the mitochondrial genomes of fungi: Here today, gone tomorrow? Mitochondrial DNA Part A. 30, 573–584. https://doi.org/10.1080/24701394.2019.1580272.

Wallis, C.M., Chen, J., de Leon, A.A.P., 2022. Mitochondrial genome resource of a drapevine strain of *Trichoderma harzianum*, a potential biological control agent for fungal canker diseases. PhytoFrontiersTM. https://doi.org/10.1094/PHYTOFR-08-21-0052-A.

Yuan, X.-L., Mao, X.-X., Liu, X.-M., Cheng, S., Zhang, P., Zhang, Z.-F., 2017. The complete mitochondrial genome of *Engyodontium album* and comparative analyses with *Ascomycota* mitogenomes. Genet. Mol. Biol. 40, 844–854. https://doi.org/10.1590/1678-4685-gmb-2016-0308.

Zhang, D., Gao, F., Jakovlić, I., Zou, H., Zhang, J., Li, W.X., Wang, G.T., 2020. PhyloSuite: An integrated and scalable desktop platform for streamlined molecular sequence data management and evolutionary

phylogenetics studies. Mol. Ecol. Resour. https://doi.org/10.1111/1755-0998.13096.

Zhang, S., Zhang, Y.-J., 2019. Proposal of a new nomenclature for introns in protein-coding genes in fungal mitogenomes. IMA Fungus. 10, 15. https://doi.org/10.1186/s43008-019-0015-5.

Zhang, Y., Wang, S., Li, H., Liu, C., Mi, F., Wang, R., Mo, M., Xu, J., 2021. Evidence for persistent heteroplasmy and ancient recombination in the mitochondrial genomes of the edible yellow chanterelles from Southwestern China and Europe. Front. Microbiol. 12, 699598. https://doi.org/10.3389/fmicb.2021.699598.

Zhang, Y., Zhang, S., Zhang, G., Liu, X., Wang, C., Xu, J., 2015. Comparison of mitochondrial genomes provides insights into intron dynamics and evolution in the caterpillar fungus *Cordyceps militaris*. Fungal Genet. Biol. 77, 95–107. https://doi.org/10.1016/j.fgb.2015.04.009.

Tables

Table 1. Mitogenome summary of *T. afroharzianum* TR37

Gene	Strand	Start position	Stop position	Length	Start codon	Stop Codon	Intergenic length	Anti codon	Note
trnR	H	85	155	71			334	UGC	
nad4L	H	489	758	270	ATG	TAA	0		
nad5	H	758	2749	1992	ATG	TAA	393		
cob	H	3142	4311	1170	ATG	TAA	113		
trnC	H	4424	4495	72			488	CGU	
cox1	H	4983	7820	1593	ATG	TAA	99		CDS (4983-5200; 6446-7820)
trnR	H	7919	7989	71			344	AGA	
nad1	H	8333	9442	1110	ATG	TAA	177		
nad4	H	9619	11073	1455	ATG	TAA	481		
atp8	H	11554	11706	147	ATA	TAA	119		
atp6	H	11825	12607	783	ATG	TAA	582		
rrnS	H	13189	14690	1502			41		
trnY	H	14731	14814	84			94	CAU	
trnD	H	14908	14981	74			6	CAG	
trnS	H	14987	15070	84			5	CGA	
trnN	H	15075	15146	72			46	CAA	
cox3	H	15192	16001	810	ATG	TAA	63		
trnG	H	16064	16134	71			110	AGG	
nad6	H	16244	16996	753			61		
trnW	H	17057	17128	72			54	AGU	
trnP	H	17182	17253	72			348	ACC	
rrnL	H	17601	23022	5422			5		
rps3	H	20968	22350	1383					
trnT	H	23027	23097	71			6	ACA	
trnE	H	20103	23175	73			1	AAG	
trnM	H	23176	23251	76			141	GUA	
trnM	H	23392	23464	73			5	GUA	
trnL	H	23469	23551	83			91		
trnA	H	23642	23713	72			6	ACG	
trnF	H	23719	23791	73			93	CUU	
trnK	H	23884	23956	73			74	AAA	
trnL	H	24030	24113	84			75	AUC	
trnQ	H	24188	24260	73			331	AAC	
trnH	H	24591	24664	74			98	CAC	
trnM	H	24762	24883	72			36	GUA	
nad2	H	24919	26586	1668	ATG	TAA	1		
nad3	H	26587	27000	414	ATG	TAA	188		
atp9	H	27188	27412	225	ATG	TAA	958		
cox2	H	28370	28816	447	ATG	TAA	36		
Homing endonuclease	H	5202	6173	972	GAC	TAA			GIY-YIG
	H	18995	19609	615	ATT	TAA			LAGLIDADG
	H	27513	28175	663	ATG	TAA			LAGLIDADG
Group I Intron (subtype of IB)		5201	6445	1245					
Group I Intron		18993	19887	895					

(subtype of IB)									
Group I Intron (subtype of IA)		20768	22408	1641					
Group I Intron (subtype of IC2)		27635	27856	232					

Other features	Value
Mitochondrial genome size (bp)	29517
AT content (%) /GC content (%)	72.33 (A, 36.10%; T, 36.23%) / 27.67 (G, 15.16%; C, 12.51%)
AT-skew/GC-skew	-0,0018 / 0.0962
Intergenic region (%)	20.68%
two rRNAs + 22 tRNAs	29.01%

Table 2. Nucleotide composition of the mitogenomes of *T. afroharzianum* strains

Feature	Strains of *T. afroharzianum*	T%	C%	A%	G%	A+T%	AT-skew	GC-skew
Whole genome	TR37	36.23	12.51	36.10	15.16	72.33	-0.0018	0.0958
	TR43	36.23	12.50	36.11	15.16	72.34	-0.0017	0.0962
	TR47	36.21	12.52	36.10	15.17	72.31	-0.0015	0.0957
PCGs	TR37	39.05	13.08	33.27	14.60	72.32	-0.0799	0.0551
	TR43	39.06	13.08	33.24	14.63	72.30	-0.0806	0.0560
	TR47	39.05	13.11	33.22	14.62	72.27	-0.0807	0.0547
PCGs-First codon position	TR37	32.44	9.60	32.77	25.18	65.21	0.0049	0.4478
	TR43	32.46	9.57	32.74	25.24	65.19	0.0042	0.4501
	TR47	32.44	9.65	32.70	25.21	65.14	0.0039	0.4463
PCGs-Second codon position	TR37	44.67	19.29	21.47	14.56	66.15	-0.3507	-0.1398
	TR43	44.67	19.29	21.47	14.57	66.14	-0.3507	-0.1392
	TR47	44.67	19.30	21.46	14.57	66.13	-0.3509	-0.1398
PCGs-Third codon position	TR37	40.02	10.33	45.59	4.05	85.62	0.0651	-0.4368
	TR43	40.06	10.36	45.55	4.04	85.60	0.0642	-0.4391
	TR47	40.03	10.37	45.50	4.09	85.54	0.0640	-0.4340
tRNAs	TR37	32.70	17.40	27.50	22.40	60.20	-0.0864	0.1256
	TR43	32.70	17.40	27.50	22.40	60.20	-0.0864	0.1256
	TR47	32.70	17.40	27.50	22.40	60.20	-0.0864	0.1256
rRNAs	TR37	31.90	12.00	38.80	17.20	70.70	0.0975	0.1781
	TR43	31.90	12.00	38.80	17.20	70.70	0.0975	0.1781
	TR47	32.00	12.10	39.00	16.90	71.00	0.0986	0.1655

Figures

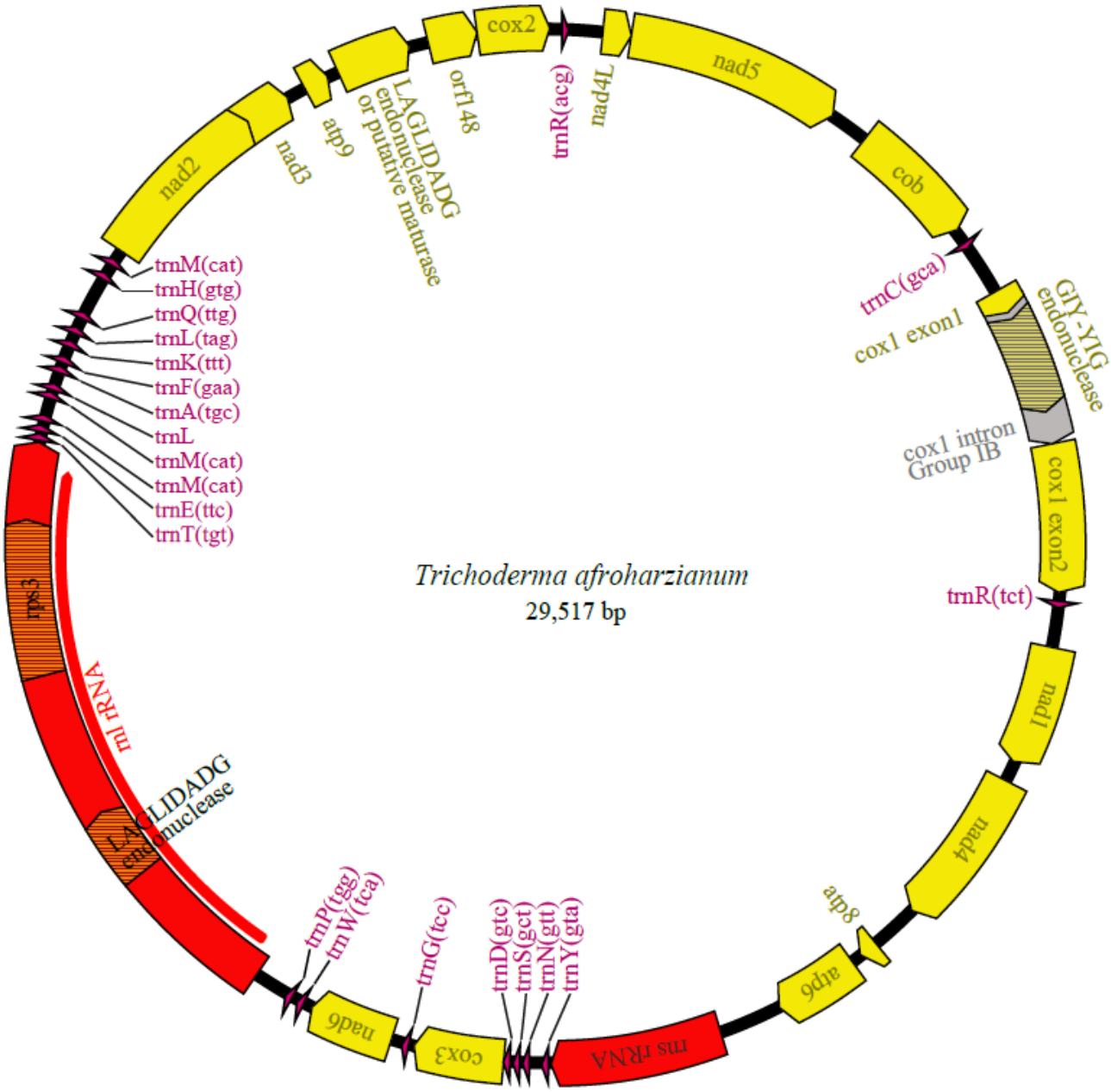

Figure 1

Circular map of the complete mitochondrial genome of *T. afroharzianum*TR37 strain. All genes are located on the heavy strand (H-strand) and transcribed in the clockwise direction. Gene clusters were shown with different colour blocks.

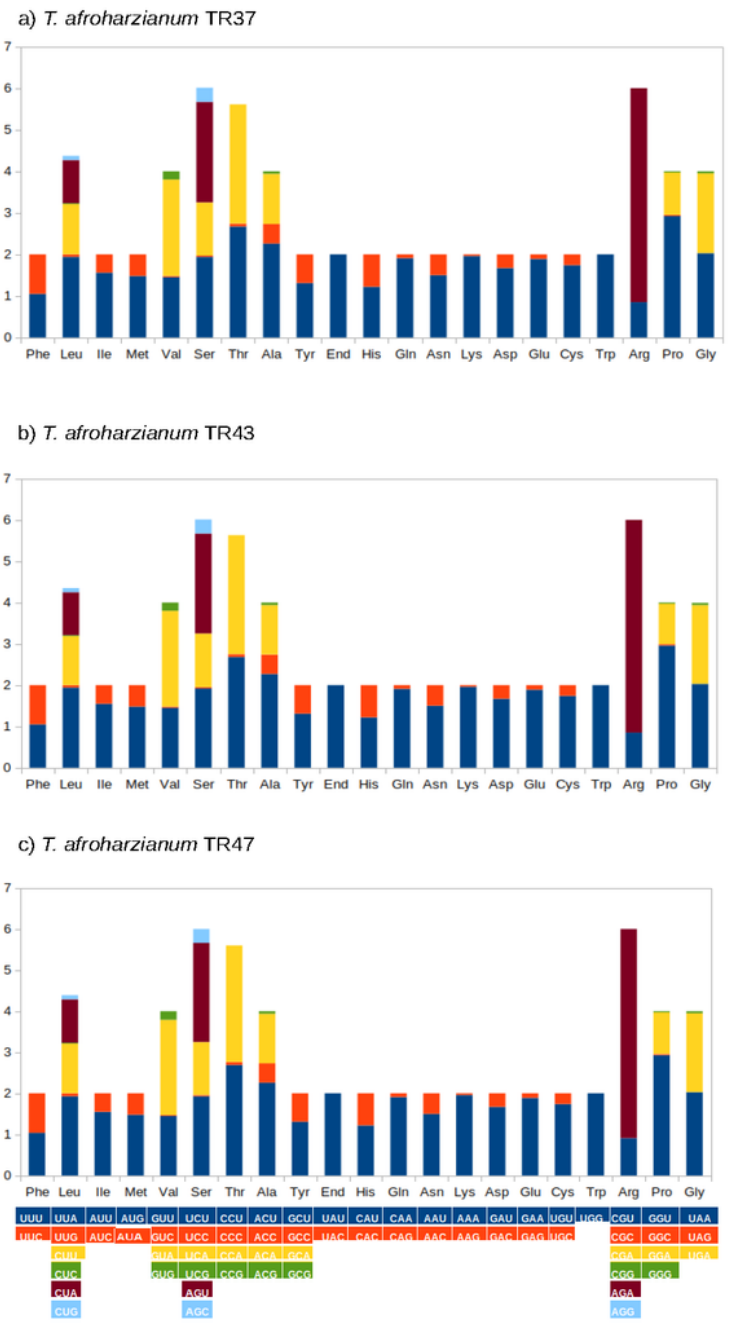

Figure 2

Relative synonymous codon usage (RSCU) of the *T. afroharzianum*mitogenomes. Codon families are provided on the x axis. The stop codons are not given.

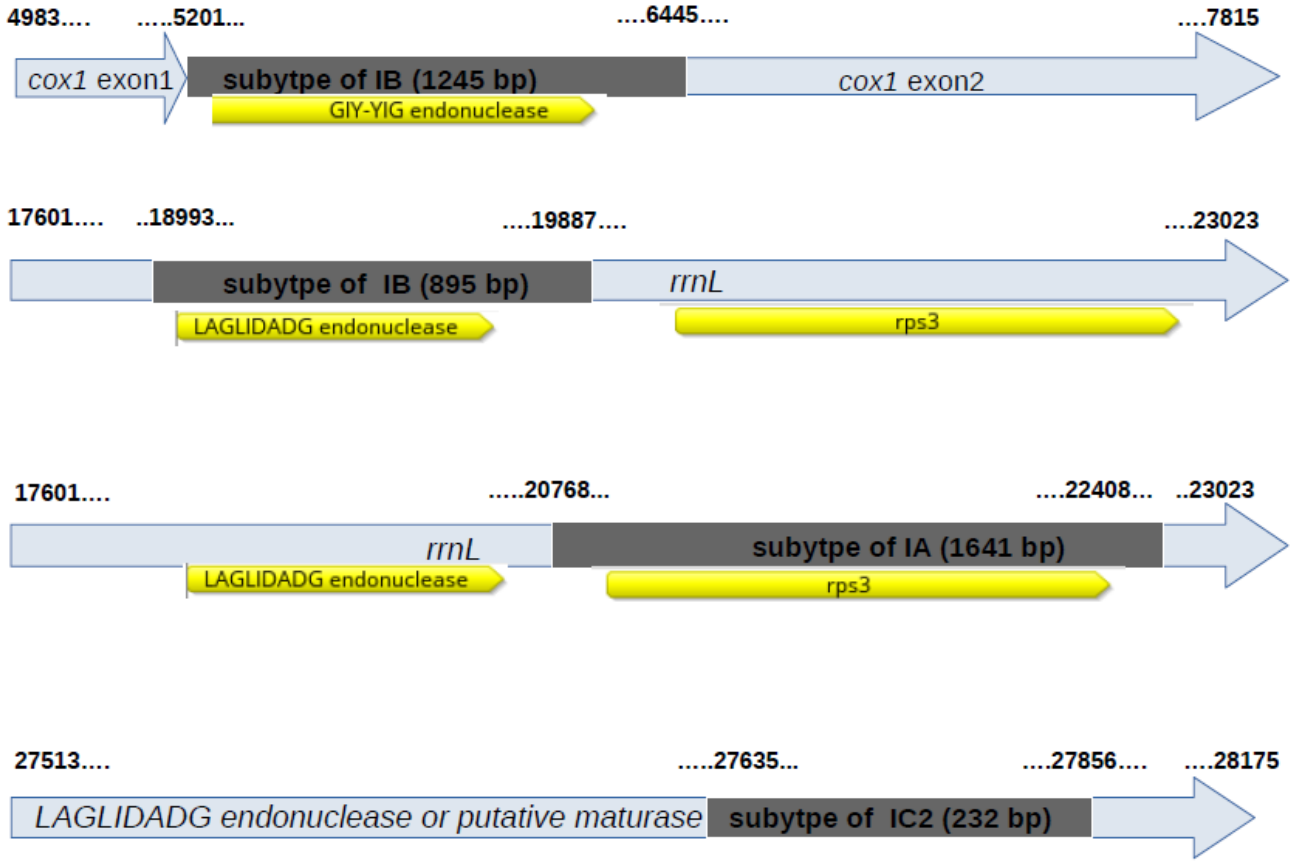

Figure 3

Schematic representation of four introns belonging to the group I intron predicted in the mitogenomes of *T. afroharzianum* TR37 strain. The predicted introns were shown with dark grey colour.

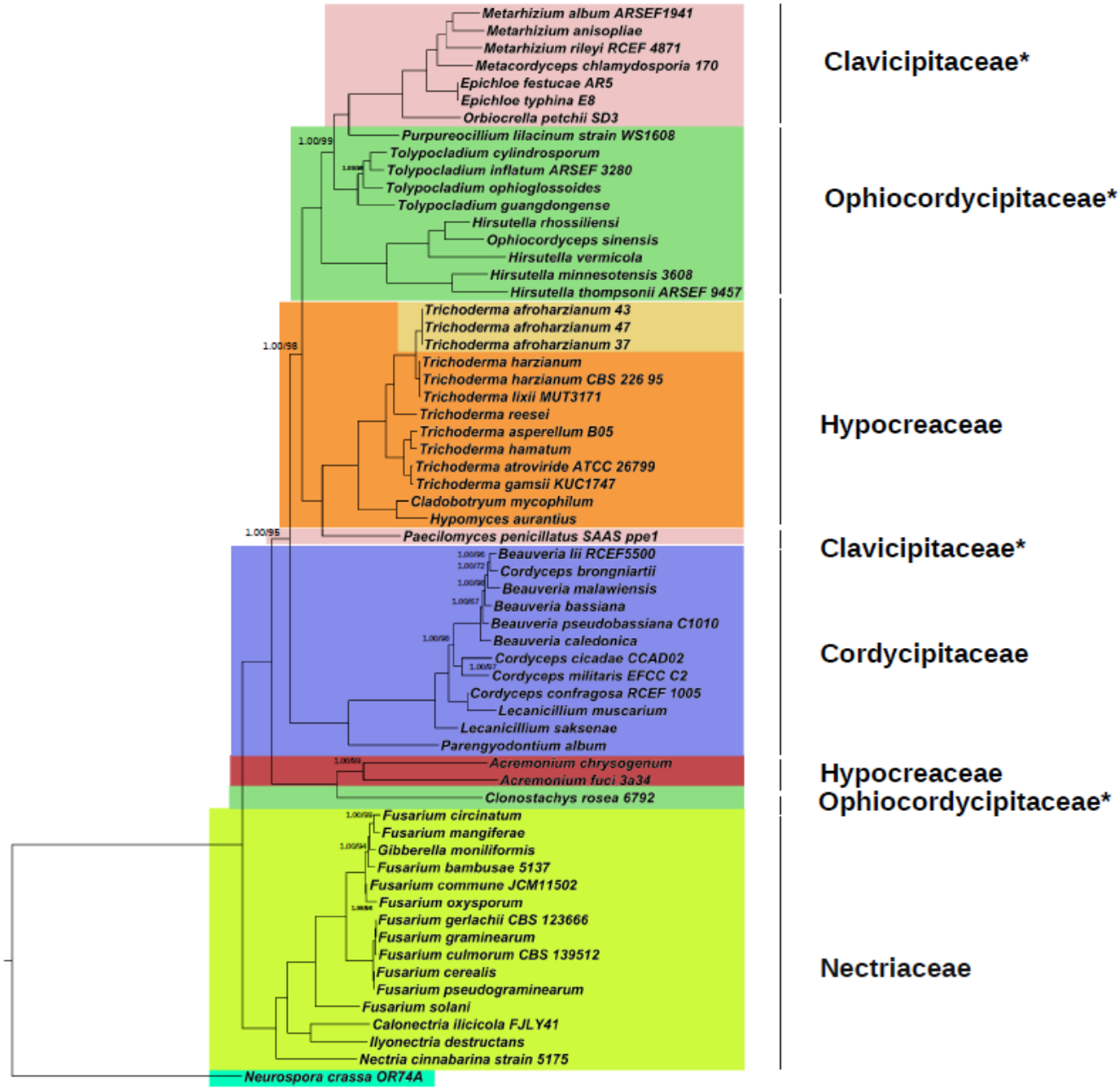

Figure 4

Phylogenetic tree of Hypocreales constructed under BI and ML approaches using a concatenated dataset of 14 mitochondrial protein coding genes; both analyses generated the same tree topology. *Neurospora crassa* (strain OR74A) (Sordariales) used as an outgroup. Support values lower than 100% in ML and 1.0 in BI were shown.

Supplementary Files

This is a list of supplementary files associated with this preprint. Click to download.

- SupplementaryFiles.docx